Clays and Clay Minerals, Vol. 55, No. 1, 45–58, 2007.

THE NATURE OF STRUCTURE-BONDED H_2O IN ILLITE AND LEUCOPHYLLITE FROM DEHYDRATION AND DEHYDROXYLATION EXPERIMENTS

VICTOR A. DRITS[1] AND DOUGLAS K. MCCARTY[2,*]

[1] Geological Institute of the Russian Academy of Science, Pyzevskij per. D.7, 109017 Moscow, Russia
[2] Chevron ETC, 3901 Briarpark, Houston, TX, 77063, USA

Abstract—Thermogravimetric analysis combined with mass spectrometry was used to study H_2O bound to samples of illite-1*M*, illite-2M_2 and leucophyllite-1*M*. Samples were heated in a helium atmosphere at different temperatures and after heating at each given temperature were cooled to 35ºC. Each cycle in the mass 18 spectrum of each illite sample contains a low-temperature peak at 60−80ºC, a medium-temperature peak at 340−360ºC, and a high-temperature peak at a temperature that is very close to the maximum temperature of sample heating of a given cycle. Within each heating-cooling cycle, the sample weight at the beginning of cooling is lower than that at the end of the same cooling stage because of H_2O resorption. However, the number of H_2O molecules released during each medium-temperature heating cycle is equal to the number of H_2O molecules resorbed during the corresponding cooling stages.

The weight losses, under medium-temperature heating, of the illite samples are related to dehydration when H_2O molecules located in K-free sites of the illite interlayers are removed. The medium-temperature peak is reproducible for each cycle because during each cooling stage the illite interlayers resorb the same number of H_2O molecules that were lost during the preceding dehydration.

Two distinct features are characteristic of leucophyllite during heating-cooling treatments. First, the number of H_2O molecules resorbed during cooling is significantly greater than the number of H_2O molecules lost during dehydration. Second, the medium-temperature peaks in the spectrum appear only in the last five cycles and the maximum-peak temperature is 450−460ºC. These data indicate that the heating-cooling treatments are accompanied by partial rehydroxylation. This rehydroxylation occurs during each cooling stage when a small number of resorbed H_2O molecules are trapped in the interlayers, although most migrate into the octahedral sheet of the 2:1 layers and reform as OH groups. The crystal chemical factors responsible for the dehydration and rehydration as well as for the rehydroxylation reactions are discussed and speculation about the origin of the low- and medium-temperature H_2O losses is presented.

Key Words—Dehydroxylation, Illite 1*M*, Illite 2M_2, Leucophyllite, Thermogravimetric.

INTRODUCTION

The dehydration and dehydroxylation of Al-rich dioctahedral 2:1 layer silicates have been studied extensively by many workers (Jonas and Grim, 1957; Mackenzie, 1957, 1982; Heller *et al.*, 1962; Slonimskaya *et al*., 1978; Heller-Kallai and Rozenson, 1980; Tsipursky *et al*., 1985; Koster van Groos and Guggenheim, 1987, 1990; Guggenheim, 1990; Bish and Duffy, 1990; Emmerich *et al*., 1999; Muller *et al*., 2000a, 2000b, 2000c; Ferrage *et al*., 2005). The processes have attracted attention for several reasons. Heating of dioctahedral 2:1 layer silicates reveals that different types of H_2O are bound in the structure. Dehydration and dehydroxylation change the physical properties of the material and the result may be useful for industrial purposes. The interpretation of the modified properties as well as the mechanism of the reactions requires a comprehensive understanding of the structural changes of dioctahedral 2:1 layer silicates in their dehydrated and dehydroxylated states.

* E-mail address of corresponding author:
dmccarty@chevron.com
DOI: 10.1346/CCMN.2007.0550104

Studies of dioctahedral micas (illite, leucophyllite, glauconite and celadonite) and smectite (montmorillonite, beidellite, nontronite) show that these minerals are characterized by a wide range of dehydroxylation temperatures (Jonas and Grim, 1957; Grim, 1968; Mackenzie, 1957). Different montmorillonite and illite types may each be classified into two groups: often referred to as 'normal' and 'abnormal' varieties. Normal montmorillonite and abnormal illite lose hydroxyl groups at 650−700ºC (Mackenzie *et al*., 1949) whereas dehydroxylation temperatures of normal illite and abnormal montmorillonite occur at 500−550ºC. Some dioctahedral 2:1 clay minerals rehydroxylate by cooling in a stream of water vapor after dehydroxylation. Jonas (1955) found that normal montmorillonite shows a peak on its differential thermal analysis (DTA) curve at ~700ºC and yields a compound showing a peak at ~550ºC on rehydroxylation of the natural sample. Heller *et al*. (1962) suggested that the ability of dioctahedral 2:1 clay minerals to rehydroxylate depends on the degree of Al-for-Si substitution in the tetrahedral sheets: montmorillonite rehydroxylated readily, nontronite only slightly, and beidellite not at all. Detailed structural investigations aided in the interpretation of these empirical observations.

The dehydroxylated structure of pyrophyllite was determined by Wardle and Brindley (1972), muscovite dehydroxylate by Udugawa *et al*. (1974) and the dehydroxylation process was interpreted by Guggenheim *et al*. (1987) using Pauling's rules. Drits *et al*. (1995) showed that the different dehydroxylation temperatures of illite and smectite are determined by the distribution of octahedral cations over *cis*- and *trans*-sites in the 2:1 layers of these minerals. For 2:1 layers of normal illites and abnormal montmorillonite, *trans*-octahedra are vacant whereas in the 2:1 layers of abnormal illites and normal smectites, one of two symmetrically independent *cis*-octahedra are vacant. The two-stage structural transformation of *cis*-vacant illite and smectite during dehydroxylation, as well as the main factors responsible for the high dehydroxylation temperature of these minerals, were discovered by Drits *et al*. (1995) and Drits (2003).

Dioctahedral 2:1 clay minerals heated at $T > 105$ºC release 'excess' H_2O in comparison with the number of OH groups in their structure. This H_2O excess probably originates from H_2O molecules bonded to the outer surfaces and within the interlayers of the mineral structures (Hower and Mowatt, 1966). Because the H_2O is bound in different ways to the 2:1 clay minerals, H_2O loss can occur over overlapping temperatures. Therefore, the characterization of differently bound H_2O may be difficult. Thus, the calculation of structural formulae based on the assumption that a framework of the 2:1 phyllosilicates consists of $O_{10}(OH, F, Cl)_2$ per half unit-cell may not be accurate. The content of adsorbed and structural H_2O in different clay minerals must be determined carefully. In particular, various cation-exchanged montmorillonite samples lost interlayer H_2O at temperatures of $\leqslant$200ºC (Koster van Groos and Guggenheim, 1987, 1990). The nature of the excess H_2O, and in general the different behavior between the various types of H_2O in illite of different chemical composition, remains poorly understood. Slonimskaya *et al*. (1978) developed a method to quantify molecular H_2O and OH groups bound to Al-rich illite-1*M*, illite-2M_1 and illite-2M_2. The samples were subjected to several heating-cooling cycles at different temperature intervals in a He atmosphere. The number of molecular H_2O and OH groups in the illite interlayers and 2:1 layers respectively, were determined. The results obtained present strong evidence that H_2O molecules exist in 'vacant' illite interlayer sites. The dehydration of interlayer H_2O in the illite samples occurs at 280−300ºC and the reaction is reversible. The paper by Slonimskaya *et al*. (1978) was published in Russian and their approach and results are not widely known by western readers.

In this work, we use a thermogravimetric technique and a modified approach developed by Slonimskaya *et al*. (1978) to investigate the thermal behavior of illite and leucophyllite samples having contrasting chemical compositions.

EXPERIMENTAL

Dehydration and dehydroxylation reactions and weight loss *vs*. sample heating were performed using a TA Instruments model 2050 thermogravimetric analysis device with a heated capillary tube. To record the atomic mass signal of evolved gas during heating the tube was connected to a ThermoOnix quadropole mass spectrometer. Reagent grade He was used as a carrier gas under positive pressure during the heating and cooling cycles. This equipment allows the weight loss owing to the release of different molecules (H_2O, OH, CO, CO_2, *etc*.) to be estimated at a given temperature.

First, a non-treated sample is heated in a He atmosphere to 300ºC at the rate of 5ºC/min, then cooled to 35ºC and allowed to equilibrate at this temperature. Next, the treatment includes two cycles: first, heating of a sample to 400ºC at 5ºC/min, cooling and equilibration at 35ºC and, second, repeating the same procedure. In each next heating stage, the temperature is increased by 50ºC and the heating-cooling procedure is repeated twice. Two additional experiments were carried out, one with a slower heating rate of 2ºC/min. The other, with delays in cooling by having the temperature held for 1 or 2 h at different temperatures. During these heating-cooling cycles the sample in the furnace chamber is purged with He (~15 cm^3/min). Weight loss is determined by the sampling interval equal to 2.0 s/pt with an error in weight believed to be <0.0001 mg and precision at ±0.05ºC.

In the Slonimskaya *et al*. (1978) procedure, a sample is heated in He to a set temperature and maintained at this temperature until the sample weight achieves a constant value. Helium is then passed over the sample, followed by cooling in He. Additional heating is performed at the same or higher temperature. The sample is maintained at this temperature until the weight achieves a constant value and then He treatment/cooling proceeds again. The main difference between the technique used in this study and that used by Slonimskaya *et al*. (1978) is that in the latter experiments, sample weight was brought to a constant value at a given temperature whereas in the present work constant heating and cooling rates were used.

SAMPLES

Two dioctahedral 2:1 layer-silicate minerals were investigated: illite and leucophyllite. The two illite samples are from hydrothermally altered volcanic rocks located near a gold-bearing mining district at Belgorod, Low Amur, Russia (Slonimskaya *et al*., 1978). The leucophyllite sample is from a salt-bearing deposit at Inder, Russia (Sokolova *et al*., 1976). Both illite samples are pure and X-ray diffraction (XRD) patterns using CuKα radiation obtained from oriented specimens contain a nearly rational series of basal reflections (Figure 1).

Simulation of the experimental XRD patterns from glycolated specimens (Figure 2) shows that both illite samples consist of interstratified illite (90%) and smectite (10%) layers and differ from each other by the mean number of layers ($\bar{N}$) in coherent scattering domains (CSDs), equal to 19 and 23, respectively. Random powder XRD patterns (CuKα radiation) show that one sample is a 1*M* structure whereas the other is a $2M_2$ structure (Figure 3). Table 1 compares the experimental and calculated *d*(*hkl*) values for illite-1*M* and $2M_2$ samples and their unit-cell parameters. Simulation of the experimental XRD pattern from the glycolated leucophyllite specimen shows that its structure consists of 92% leucophyllite and 8% smectite layers with $N = 9$ (Figure 2). The powder XRD pattern of the leucophyllite sample shows that it has the 1*M* structure (Figure 3, Table 1). In addition, the sample contains 0.5% quartz and 0.7% anatase. The values of ccosβ/*a* calculated from the unit-cell parameters (Table 1) indicate that the structures of illite-1*M* and illite-$2M_2$ and leucophyllite-1*M* consist of *trans*-vacant (*tv*) 2:1 layers (Bailey, 1984). Table 2 presents chemical analyses of the studied samples. The structural formulae for the illite-1*M* and illite-$2M_2$ are: $K_{0.74}Na_{0.03}(Al_{1.91}Fe^{3+}_{0.01}Ti_{0.01}Mg_{0.09})(Si_{3.22}Al_{0.78})O_{10}(OH)_2$ and $K_{0.74}Ca_{0.03}Na_{0.01}(Al_{1.99}Ti_{0.01})(Si_{3.18}Al_{0.82})O_{10}(OH)_2$, respectively. For the leucophyllite-1*M*, the structural formula is: $K_{0.65}Ca_{0.03}Na_{0.01}(Al_{1.18}Fe^{3+}_{0.25}Fe^{2+}_{0.01}Mg_{0.59})(Si_{3.80}Al_{0.20})O_{10}(OH)_2$. These formulae show that both illite samples have a high substitution of Al for Si and

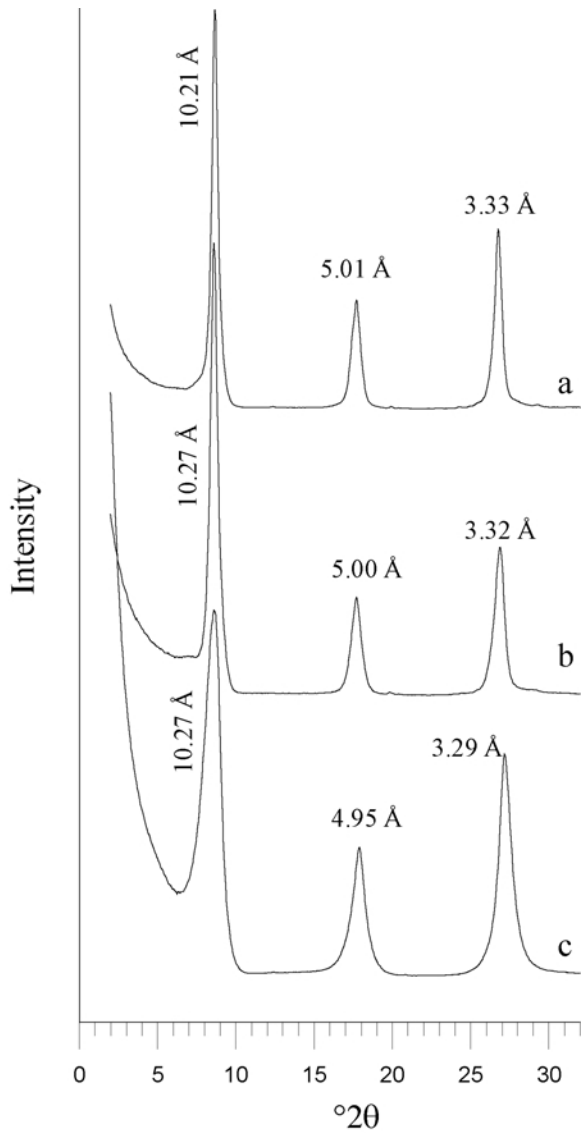

Figure 1. XRD patterns from oriented illite-$2M_2$ (a), illite-1*M* (b) and leucophyllite (c) samples collected from an air-dried state (CuKα radiation).

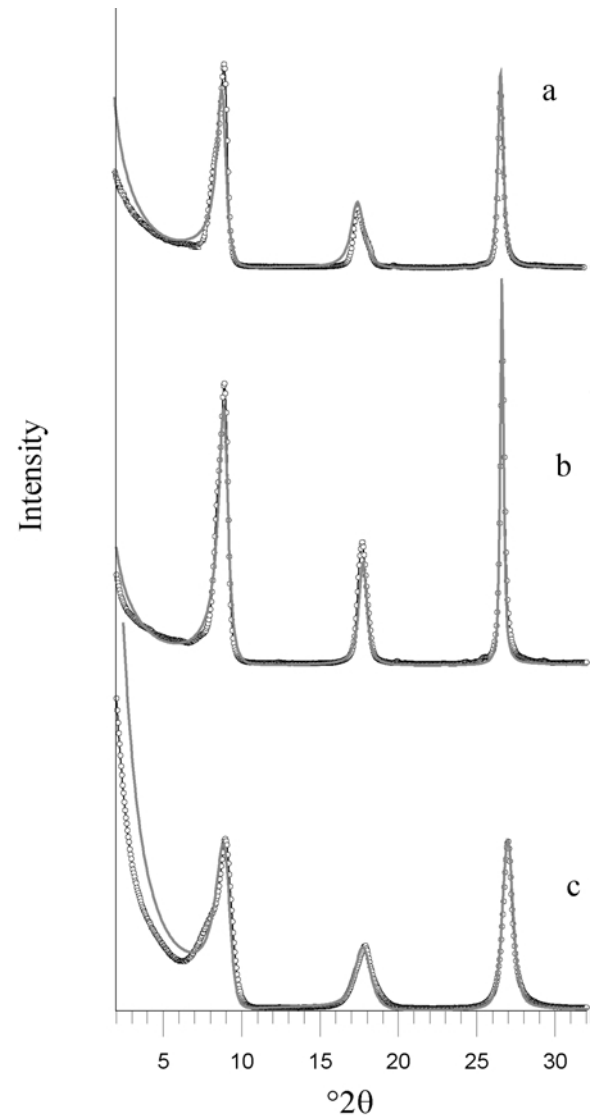

Figure 2. Experimental and calculated XRD patterns from oriented and glycolated illite-$2M_2$ (a), illite-1*M* (b) and leucophyllite (c) samples, which contain 10%, 10% and 8% smectite layers and 23, 19 and 9 layers in coherent scattering domains (CSD), respectively.

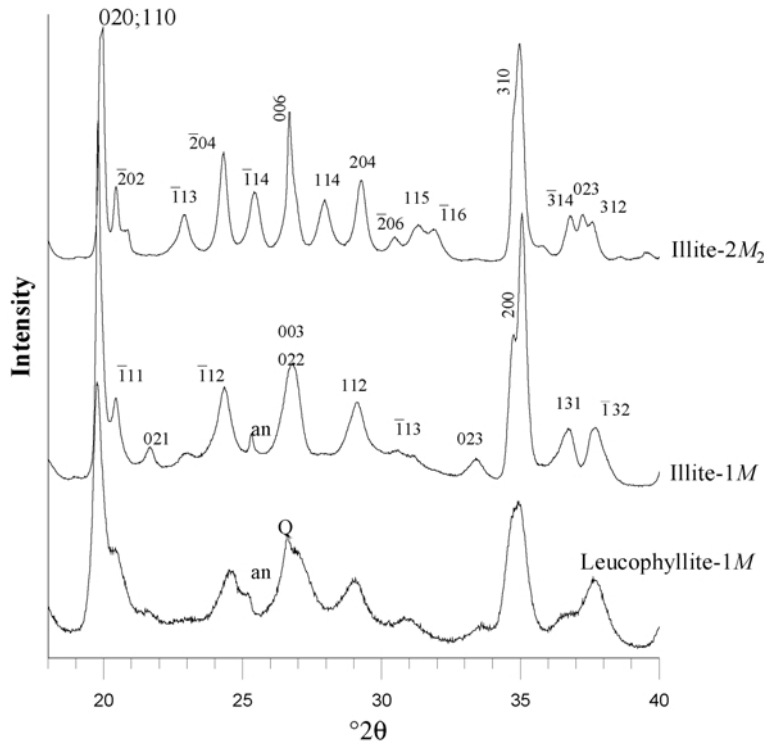

Figure 3. Random powder XRD patterns of illite-2M_2, illite-1M and leucophyllite-1M samples showing diagnostic *hkl* indices (an = anatase, Q = quartz).

the octahedral sites are occupied principally by Al in the illite-2M_2 sample or contain 0.06 cations of Mg per $O_{10}(OH)_2$ in the illite-1M sample. In contrast, the leucophyllite sample has a low substitution of Al for Si, but a large octahedral Mg content.

RESULTS

Figure 4 shows the mass 18 spectra of H_2O that evolved thermally from the studied samples. The maximum value of each peak corresponds to the temperature where the maximum rate of weight loss

Table 1. Indexing and comparison of the experimental and calculated *d* values (Å) of *hkl* reflections in the powder XRD patterns from illite-1*M*, leucophyllite-1*M* and illite-2M_2 samples.

Illite-1*M*			Leucophyllite-1*M*		Illite-2M_2		
hkl	d_{exp}	d_{cal}	d_{exp}	d_{cal}	*hkl*	d_{exp}	d_{cal}
020	4.480	4.500	4.489	4.497	110	4.454	4.448
110		4.447		4.458	$\bar{2}02$	4.341	4.348
$\bar{1}11$	4.341	4.355	4.33	4.312	$\bar{1}12$	4.251	4.270
021	4.100	4.102	4.11	4.095	$\bar{1}13$	3.884	3.881
$\bar{1}12$	3.654	3.654	3.621	3.620	$\bar{2}04$	3.657	3.661
022	3.324	3.324	3.317	3.323	$\bar{1}14$	3.501	3.497
003	3.324	3.324		3.310	006	3.336	3.337
112	3.064	3.064	3.074	3.074	114	3.189	3.190
$\bar{1}13$	2.923	2.921	2.894	2.890	204	3.048	3.049
023	2.681	2.676	2.665	2.662	$\bar{2}06$	2.930	2.933
130	2.582	2.587			115	2.854	2.854
$\bar{1}31$			2.566	2.565	$\bar{1}16$	2.806	2.800
200	2.557	2.557			310	2.563	2.563
131	2.444	2.445	2.446	2.449	$\bar{3}14$	2.442	2.442
$\bar{1}32$	2.390	2.388	2.389	2.389	023	2.411	2.413

Unit-cell parameters:	*a* (Å)	*b* (Å)	*c* (Å)	β (º)	*c*cosβ (º)/*a*
illite-1*M*	5.222(4)	9.000(6)	10.19(1)	101.6(1)	−0.394
leucophyllite-1*M*	5.226(8)	9.000(10)	10.09(2)	100.8(1)	−0.363
illite-2M_2	8.992(6)	5.176(3)	20.36(1)	100.5(1)	−0.413

Table 2. Chemical analyses (wt.%) of the studied samples.

Sample	SiO_2	TiO_2	Al_2O_3	Fe_2O_3	FeO	MgO	CaO	Na_2O	K_2O	H_2O^-	H_2O^+
Illite-1*M*	48.62	0.30	34.48	0.16	0.10	0.91	0.03	0.06	8.80	1.12	5.13
Illite-2M_2	48.06	0.15	38.01	0.13	0.10		0.40	0.05	8.76	1.18	5.08
Leucophyllite-1*M*	55.93	0.70	17.11	4.85	0.16	5.73	0.44	0.07	7.44	2.93	5.42

In the leucophyllite-1*M*, the SiO_2 value was decreased by 0.5% from the measured value to account for the quartz impurity.

occurs. The number of peaks, their maximum values, and temperatures depend on the chemical composition of the sample, the number of expandable layers in the structure, the temperature where partial dehydroxylation occurs and other factors (see below).

Figure 4 shows the heating-cooling cycles. Each cycle starts from 35ºC and is located in the figures immediately before the set of peaks at ~60−80ºC and finishes at the peak of the maximum temperature of heating corresponding to a given cycle. The cooling starts immediately after the high-temperature peak and finishes at 35ºC immediately before the low-temperature peak at 60−80ºC of the next heating sequence. Thus, a characteristic feature of Figure 4 is that each heating-cooling cycle starts near a low-temperature peak and completes close to the next nearest low-temperature peak.

Illite-2M_2 and illite-1M

Each cycle (Figure 4a,b) in the mass 18 spectra contains a low-temperature peak at ~60−80ºC, a medium-temperature peak at 340−360ºC and a high-temperature or dehydroxylation peak. This last peak occurs at temperature that is, on average, 10ºC less than the maximum temperature of sample heating corresponding to a given cycle. When the heating temperature is <450ºC, the final peaks at 350ºC and 400ºC overlap to produce an asymmetrical shape corresponding to the first two to three cycles (Figure 4a,b).

The cooling stages of each cycle are characterized (Figure 4a,b) in the mass 18 patterns as a horizontal line although immediately after the high-temperature or dehydroxylation peak a narrow minimum occurs at 280−300ºC. Tables 3 and 4 contain sample-weight *vs*.

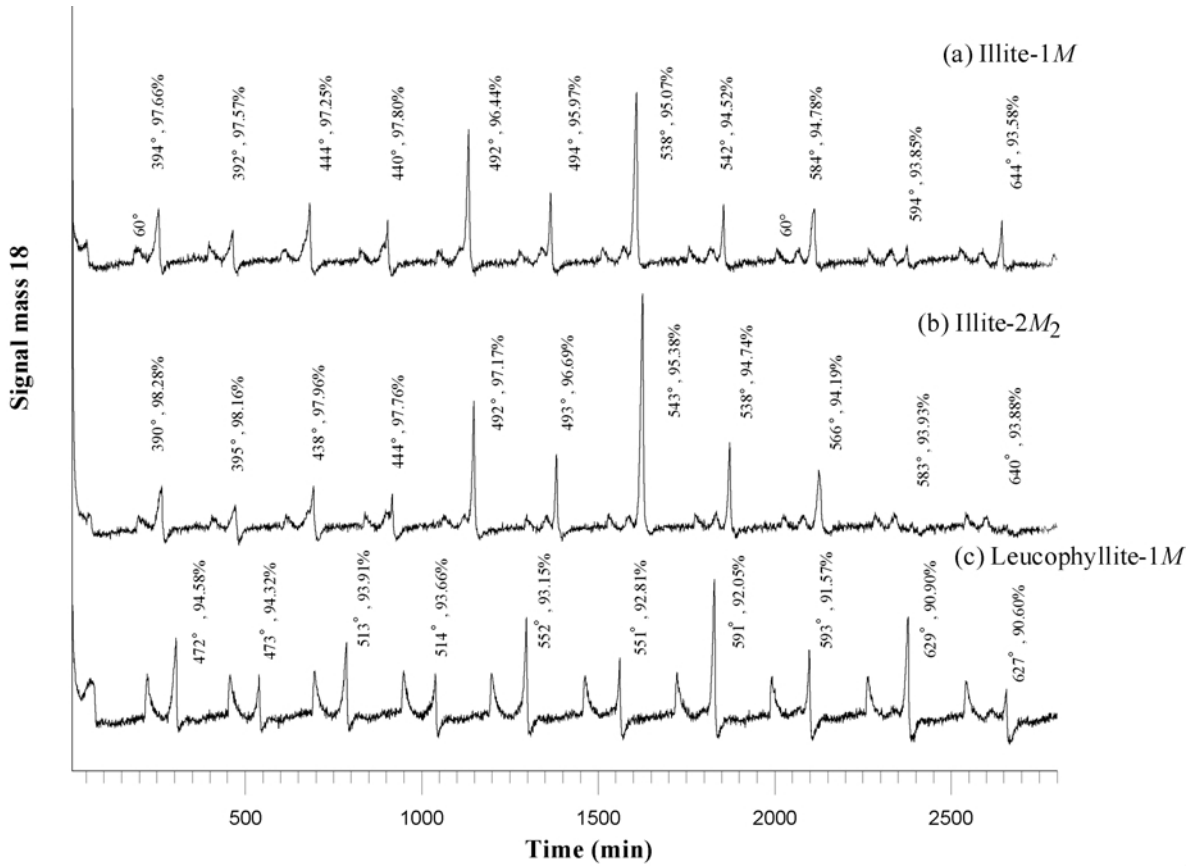

Figure 4. Mass 18 spectra representing thermally evolved water from illite-1*M*, illite-2M_2 and leucophyllite samples. The temperature of the dehydroxylation peak and the associated weight percent of the original sample weight are labeled (see text).

Table 3. Weight and temperature values for heating and cooling stages for illite and leucophyllite samples.

Cycle	Weight at T_0 (%)	T_1	Weight at T_1 (%)	T_2	Weight at T_2 (%)	T_3	Weight at T_3 (%)	T_4	Weight at T_4 (%)	Weight loss from T_0 to T_4 (%)
Illite-2M_2										
1	98.92	62.80	98.90	235.30	98.73					
2	98.48	91.59	98.43	232.00	98.38					
3	98.41	68.50	98.39	224.40	98.32	358.20	98.21	396.80	98.12	0.29
4	98.14	58.70	98.12	225.10	98.06	369.70	97.93	412.60	97.85	0.29
5	97.99	73.40	97.96	255.80	97.90	352.30	97.81	411.20	97.71	0.28
6	97.22	59.90	97.21	247.40	97.15	349.10	97.06	418.90	96.97	0.25
7	96.83	87.40	96.79	237.50	96.76	355.20	96.65	434.90	96.57	0.25
8	95.31	77.50	95.28	233.30	95.24	340.30	95.15	431.00	95.07	0.24
9	94.79	67.60	94.76	223.20	94.72	341.30	94.63	453.80	94.54	0.25
10	94.21	62.80	94.19	218.60	94.15	331.00	94.07	438.30	93.98	0.23
11	94.16	66.50	94.14	222.00	94.09	324.00	94.03	484.60	93.92	0.24
12	94.11	61.20	94.10	206.10	94.05	345.60	93.96	447.40	93.89	0.22
Illite-1M										
1	98.35	82.90	98.22	238.60	98.15					
2	97.90	75.90	97.87	238.90	97.81					
3	97.82	79.70	97.79	238.00	97.73					
4	97.48	54.70	97.47	263.80	97.39	376.40	97.27	408.60	97.19	0.29
5	97.31	85.00	97.27	213.60	97.23	352.80	97.15	415.60	97.01	0.25
6	96.53	60.70	96.52	222.00	96.46	372.30	96.34	426.10	96.25	0.28
7	96.18	77.30	94.16	238.00	96.11	361.40	96.01	431.00	95.90	0.28
8	95.05	59.00	95.03	230.2	94.98	359.80	94.88	461.60	94.78	0.27
9	94.71	52.40	94.70	229.50	94.64	369.10	94.53	471.00	94.45	0.26
10	94.20	52.90	94.19	240.90	94.13	358.80	94.04	487.50	93.95	0.25
11	94.09	60.70	94.07	227.00	94.02	355.50	93.94	510.00	93.84	0.25
12	93.79	57.80	93.77	229.00	93.72	374.10	93.62	518.90	93.56	0.23
13	93.63	55.20	93.62	232.40	93.56	350.30	93.50	521.90	93.40	0.23
14	93.34	58.00	93.32	213.50	93.27	363.80	93.19	563.80	93.12	0.22
Leucophyllite-1M										
1	95.58	60.40	95.50	169.40	95.27			358.30	95.18	0.39
2	94.97	62.42	94.89	185.30	94.67			374.10	94.61	0.37
3	94.81	59.32	94.74	187.00	94.51			385.40	94.45	0.37
4	94.35	56.26	94.30	198.10	94.06			420.10	93.96	0.41
5	94.15	56.18	94.10	174.40	93.88			439.10	93.74	0.43
6	93.57	60.20	93.50	183.00	93.29			466.10	93.10	0.48
7	93.28	58.35	93.22	185.60	93.00	445.36	92.83	468.80	92.81	0.48
8	92.47	60.48	92.40	197.80	92.20	457.17	91.99	490.20	91.96	0.52
9	92.11	62.49	92.04	190.10	91.85	444.52	91.65	492.00	91.60	0.53
10	91.37	60.88	91.31	183.60	91.12	452.62	90.90	532.80	90.82	0.56
11	91.16	53.89	91.13	200.00	90.91	455.00	90.69	573.00	90.58	0.59
12	90.90	57.87	90.86	214.00	90.65	454.15	90.45	638.00	90.28	0.62

T_0 is the temperature at which each heating stage begins; T_1 is the temperature value of the low-temperature peak; T_2 is the temperature at which the low-temperature weight loss is completed; T_3 is the temperature value of the medium-temperature peak; and T_4 is the temperature at which the medium temperature weight loss is completed (see Figure 5).

temperature values to characterize the illite-1M and 2M_2 behavior. Figure 5 shows a portion of the mass 18 spectrum of the illite-2M_2 sample to illustrate weight changes at temperatures which are characteristic for each heating-cooling cycle. Low- and medium-temperature weight losses occur from T_0 = 35ºC to T_2 and from T_2 to T_4, respectively. Dehydroxylation starts from T_4. Two important features should be noted. First, within each heating-cooling cycle, the sample weight at the high-temperature peak (T_{max}) is greater than that at T_5 ($T_5 < T_{max}$). This means that weight loss continues at the beginning of the cooling stage. Second, within each heating-cooling cycle the weight of the samples at the beginning of cooling (T_5) is less than the weight at the end of the same cooling stage at T_0. Thus, each cooling stage is accompanied by increasing sample weight from resorbing H_2O. Note that the minimum of the mass 18 spectrum which occurred at 280−300ºC during each cooling stage corresponds to the maximum rate of weight gain. Figure 6 shows the losses and increases of the sample weight after each heating and cooling stage. First, with the heating rate of 5ºC/min, sample-weight losses related to the low- and medium-temperature peaks for both illite samples are equal, on average, to

Table 4. Cooling temperature, sample weight and total weight of resorbed H_2O during cooling stages for illite and leucophyllite.

Cycle	T_5 (%)	Weight at T_5 (%)	Weight at T_6 (%)	Weight at T_0 (%)	Total weight resorbed H_2O (%)
Illite-2M_2					
1	378.65	98.21	98.40	98.48	0.27
2	374.40	98.15	98.34	98.41	0.26
3	410.60	97.87	98.06	98.14	0.27
4	425.30	97.72	97.91	97.99	0.27
5	441.80	96.97	97.15	97.23	0.25
6	434.40	96.58	96.76	96.84	0.25
7	478.40	95.07	95.23	95.32	0.24
8	497.00	94.55	94.71	94.79	0.24
9	540.90	93.97	94.13	94.21	0.24
10	565.60	93.90	94.08	94.16	0.24
Illite-1M					
1	381.90	97.61	97.80	97.90	0.30
2	371.50	97.54	97.73	97.82	0.28
3	406.60	97.18	97.39	97.48	0.30
4	403.50	97.02	97.22	97.31	0.29
5	460.60	96.25	96.44	96.53	0.29
6	446.80	95.90	96.08	96.18	0.29
7	497.30	94.78	94.95	95.05	0.28
8	504.60	94.45	94.61	94.71	0.27
9	562.40	93.94	94.10	94.20	0.26
10	583.30	93.84	94.00	94.09	0.26
11	581.00	93.55	93.71	93.79	0.24
12	618.20	93.40	93.55	93.63	0.24
13	655.22	93.10	93.25	93.34	0.24
Leucophyllite-1M					
1	467.16	94.48	94.67	94.97	0.49
2	445.00	93.30	94.51	94.81	0.52
3	483.11	93.82	94.06	94.35	0.55
4	476.00	93.63	93.87	94.15	0.54
5	520.10	93.01	93.29	93.57	0.57
6	504.50	92.72	93.00	93.28	0.57
7	536.90	91.87	92.20	92.47	0.61
8	546.00	91.51	91.84	92.11	0.62
9	583.10	90.75	91.11	91.37	0.63
10	592.00	90.54	90.90	91.16	0.64
11	572.00	90.31	90.66	90.91	0.58
12	558.00	90.37	90.01	90.25	0.54

T_5 is the temperature at which the minimal sample weight for each heating stage is achieved; T_6 = 80º for illite-1M and illite-2M_2, and is equal to 100ºC for leucophyllite.

0.07−0.08% and 0.17−0.20%, respectively, although a trend is observed where weight loss related to the medium-temperature heating decreases slightly with increasing cycle number (Figure 6a,c). Second, for all cycles, sample weight loss at the medium-temperature heating is equal to the increase in weight during cooling from the highest temperature (T_5) where the maximum weight loss observed is to 80ºC (Figure 6c,d). Similarly, weight loss related to low-temperature heating (0.07−0.08%) is equal to the increase in weight during cooling from 80 to 35ºC (Figure 6a,b). Therefore, the total increase of sample weight during cooling (0.24−0.28%) is equal to the total weight loss related to the low- and medium-temperature heating for each cycle (Tables 3, 4). Note that a minimal sample weight at the beginning of each cooling stage at T_5 equals the sample weight where the high-temperature peak starts at T_4 during the next heating cycle (Table 5, Figure 5).

For the illite-1M sample, decreasing the heating rate to 2ºC/min is accompanied by a noticeable increase in weight loss related to the medium-temperature heating. Figure 6c shows that weight losses are equal, on average, to 0.24% in contrast to a 0.17−0.20% loss when the rate was 5ºC/min. For illite-1M, weight loss related to the medium-temperature heating increases significantly when the temperature is kept at 300ºC and

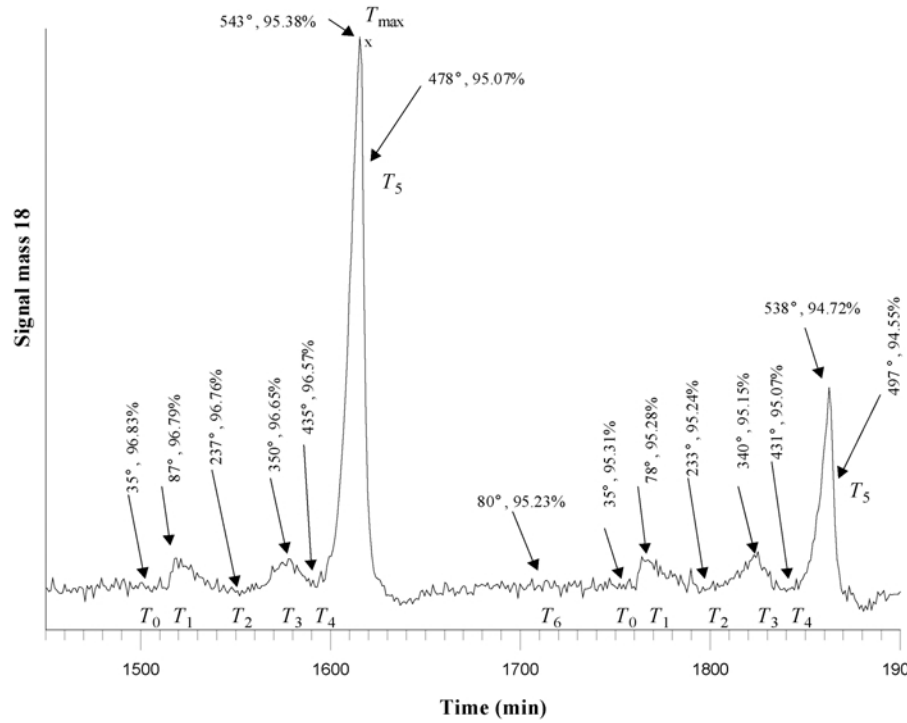

Figure 5. Portion of mass 18 spectrum showing details of two heating and one cooling stage including the point where the heating stage starts (T_0); the low-temperature peak (T_1); the point where the low-temperature weight loss ends (T_2); the medium temperature peak (T_3); the point where the medium-temperature weight loss ends (T_4); the temperature and sample wt.% at the high-temperature dehydroxylation peak (T_{max}); the point of minimum sample weight during dehydroxylation (T_5). T_6 represents the boundary between the weight increase due to H_2O sorbtion into interlayer sites (T_5 to T_6) and to the outer surfaces (T_6 to T_0) (see text).

250ºC for 1 h during each cooling stage. Figure 6c shows that under such conditions, weight losses are equal to 0.30−0.35% and decrease significantly with increasing cycle number. Similarly, for each cycle, weight loss is equal to the increase of weight during cooling from T_5 to 80ºC (Figure 6c,d).

To estimate the amount of H_2O released by dehydroxylation, weight losses caused by high-temperature heating at each cycle were summed. Table 5 contains temperatures where dehydroxylation starts and ends, the weights of 1*M* and $2M_2$ samples at these temperatures, and the weight loss owing to dehydroxylation. The number of OH groups released during the first heating is two to three times greater than the weight loss observed during the second heating at the same temperature. The greatest amount of OH loss occurs for both samples at 450−550ºC (3.74% for $2M_2$ and 3.20% for 1*M* samples, Table 5). Total weight losses from dehydroxylation are equal to 4.65% for 1*M* and 4.61% for illite-$2M_2$. These values are consistent with the structural formulae of $O_{10}(OH)_2$ per half cell and equal to 4.62% for illite.

1M leucophyllite

The thermal pattern of this sample (Figure 4c) differs significantly from those observed for illite samples. Each heating-cooling cycle displays two peaks at ~65ºC and at temperature that is very close to the maximum temperature of a given cycle. Note that the temperature of the first heating-cooling cycle was equal to 480ºC. Small peaks at ~450ºC occur only when the maximum temperatures of the heating stages are >600ºC, which occurs for the last five cycles. Tables 3 and 4 contain sample weights and temperature values for different heating-cooling cycles. Figure 6a,b and Figure 7 show the losses and increases of sample weight after each heating and cooling stage. For all heating-cooling cycles, the increase of sample weight during cooling from 100 to 35ºC is identical (0.25−0.30%) and equal to the weight loss for heating from 35ºC to 180−200ºC (Figure 6a,b). The increase and loss of weight for leucophyllite (0.24−0.31%) is three to four times greater than the corresponding values (0.07−0.10%) found for illite-1*M* and $2M_2$ samples (Figure 6a,b).

In contrast to illite-1*M* and $2M_2$, cooling of leucophyllite from T_5 (Table 4) where minimal weight loss occurs to 100ºC is accompanied by an increase in weight from 0.19−0.21% to 0.35−0.36% with an increase of cycle number (Figure 7). Similarly, the loss of weight during heating from T_2 (Table 3) to the temperature where dehydroxylation starts (T_4 in Table 3) also increases with cycle number from 0.09% to 0.37% (Figure 7). However, for each given heating stage, weight loss is significantly lower than the increase of

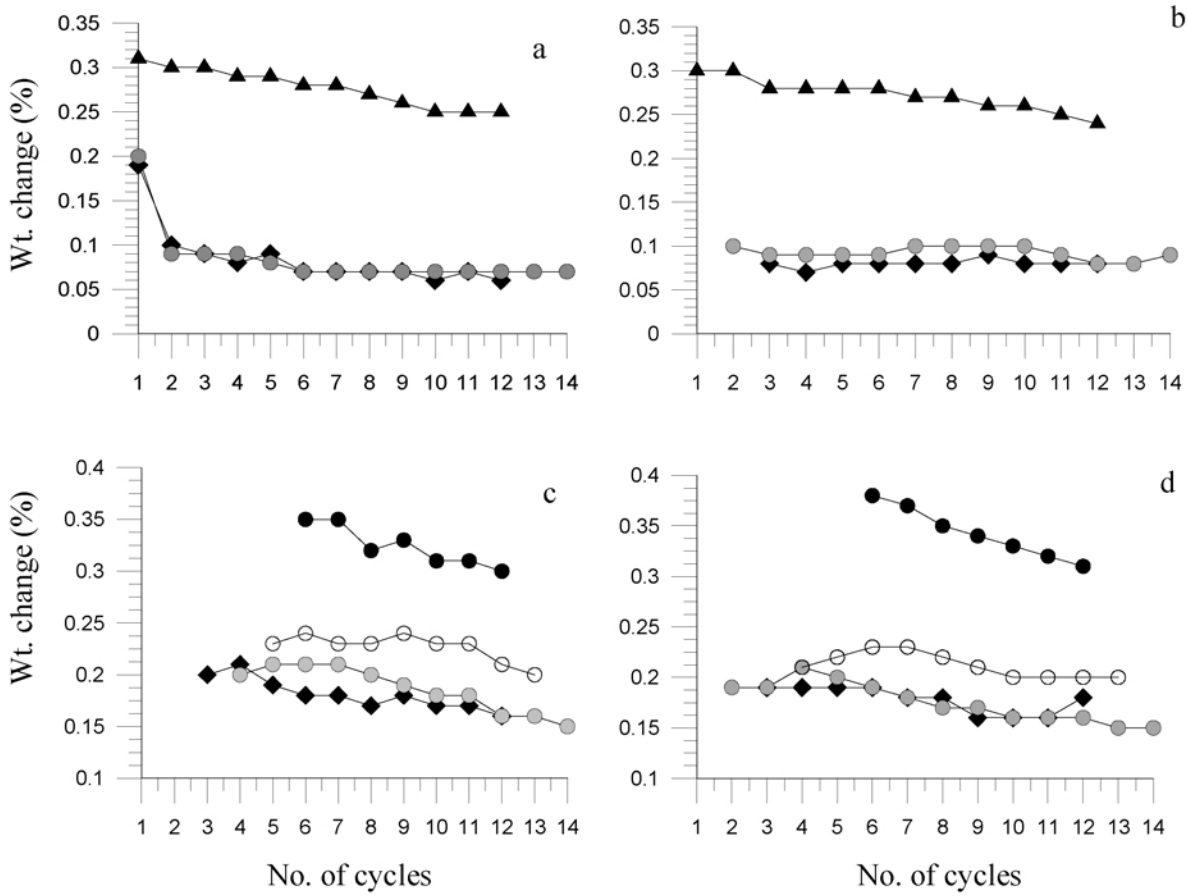

Figure 6. Weight loss and weight gain with cycle number. Weight loss during low-temperature heating (a). Weight gain during cooling from T_6 to T_0 (b). Weight loss during medium-temperature heating (c). Weight gain during cooling from T_5 to T_6 (d). Black diamond = illite-2M_2 with 5°/min heating rate; shaded circle = illite-1M with 5°/min heating rate; black triangle = leucophyllite with 5°/min heating rate. Open circle = illite-1M with 2°/min heating rate; cooling rate was the same. Black circle = illite-1M with 5°/min heating rate with slow cooling rate (see text).

weight in the preceding cooling stage (Figure 7). This difference permanently decreases with increasing cycle number and diminishes to near zero for the last two cycles (Figure 7) where the peak at 430−450ºC is observed. For these cycles, the minimal weight of leucophyllite occurs during the preceding heating-cooling cycle and this weight is close to the sample weight where the high-temperature peak of the next heating-cooling cycle starts. Note that in the leucophyllite-1M sample the maximum rate of weight increase during the cooling stage occurred at 400−420ºC and it is observed as a narrow minimum located just after the high-temperature peak on the mass 18 spectrum (Figure 4c).

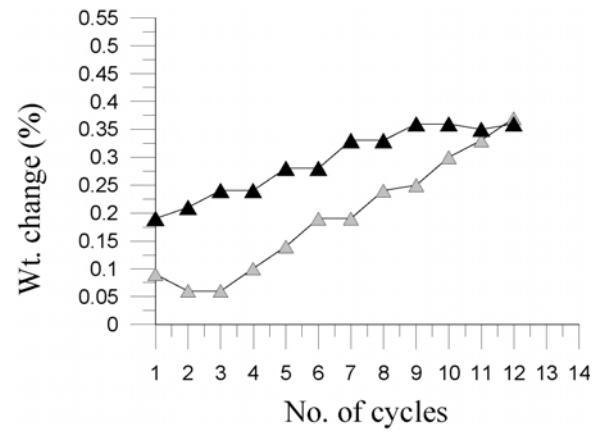

Figure 7. Weight loss (shaded triangles) during heating stages and weight gains (black triangles) during cooling stages from the leucophyllite sample.

DISCUSSION

Interlayer H_2O in illite

We suggest a mechanism of dehydration-rehydration of the illite interlayers during heating-cooling cycles. A characteristic feature of illite is that K cations occupy most but not all interlayer cavities available, with the

remaining interlayer sites probably being occupied by H_2O. In the experiment of Slonimskaya *et al*. (1978), these molecules are removed by heating at 280−300ºC, *i.e.* at temperatures which are too low to originate a rehydoxylation process. In the present experiments, the H_2O molecules are removed from the structure by heating from T_2 to T_4 (Table 3). A further increase in temperature $>T_4$ releases additional H_2O molecules by dehydroxylation and they also leave the structure. However, some H_2O molecules are resorbed during the following cooling stage. The resorbance occurs within the interval from T_5 to T_6 = 80ºC, and note T_5 increases from 400 to 600ºC with increasing cycle number.

The equality of sample weight at the end and beginning of dehydroxylation for the preceding and following heating stages (Table 5) indicates that the number of OH groups in the 2:1 layers does not change under the low- and medium-temperature treatments. The total weight losses owing to dehydroxylation determined for illite-1*M* and $2M_2$ samples (Table 5) show that dehydration does not occur simultaneously with dehydroxylation. One possible reason is that the temperatures of the medium-temperature heating are not sufficient to provide dehydroxylation. This conclusion is consistent with a correlation between Al-for-Si tetrahedral substitution in the 2:1 layers and the ability of dioctahedral phyllosilicates to rehydroxylate under mild conditions (Heller *et al*., 1962). The greater the tetrahedral Al content, the less likelihood there is of the structure rehydroxylating.

The characteristic feature of dehydration is that it is reversible. Indeed, in the illite-1*M* and $2M_2$ samples, interlayer H_2O is removed upon heating at ~340ºC and 360ºC, respectively. However, each successive heating of the samples at $T_{max}>450$ºC is accompanied by the occurrence of a medium-temperature peak at the same temperature (~340 or 360ºC) when the sample is heated again after cooling. The number of interlayer H_2O molecules removed by medium-temperature heating decreases slightly with increasing numbers of heating-cooling cycles (Figure 6c). However, during each cooling stage the illite interlayers resorb the same number of H_2O molecules lost during the preceding dehydration (Figure 6d). The trend towards fewer dehydrating and re-hydrating interlayer H_2O molecules with increasing T_{max} (Figure 6c,d) is evidence that the weight loss at

Table 5. Weight loss due to dehydroxylation.

Cycle	T_4	Sample weight at T_4 (%)	T_5	Sample weight at T_5 (%)	Dehydroxylation weight % loss
Illite-$2M_2$					
1	382.0	98.53	378.6	98.21	0.32
2	387.5	98.21	374.4	98.15	0.06
3	396.8	98.15	410.6	97.86	0.29
4	412.6	97.85	425.3	97.72	0.13
5	411.2	97.71	441.8	96.97	0.74
6	418.9	96.97	434.4	96.58	0.39
7	434.9	96.57	478.4	95.07	1.50
8	431.0	95.07	497.0	94.55	0.52
9	453.8	94.55	540.9	93.97	0.58
10	438.3	93.98	565.6	93.90	0.08
				Total hydroxyl weight	4.61
Illite-1*M*					
1	375.5	97.75	381.9	97.61	0.14
2	380.8	97.61	385.9	97.54	0.07
3	390.1	97.54	406.6	97.18	0.36
4	408.6	97.18	421.5	97.02	0.16
5	395.6	97.02	460.6	96.25	0.77
6	426.1	96.25	446.8	95.90	0.35
7	431.0	95.90	497.3	94.78	1.12
8	461.6	94.78	504.6	94.45	0.33
9	471.0	94.45	562.4	93.94	0.51
10	487.5	93.94	583.3	93.84	0.10
11	510.0	93.84	581.0	93.55	0.29
12	518.9	93.55	618.2	93.40	0.15
13	521.9	93.40	655.22	93.10	0.30
				Total hydroxyl weight	4.65

T_4 is the temperature at which the medium-temperature weight loss is completed; T_5 is the temperature at which the minimal sample weight for each heating stage is achieved (see Figure 5).

medium-temperature heating is related to dehydration, but not rehydroxylation. Indeed, dehydroxylation during heating-cooling cycles may be related to rehydroxylation. However, if rehydroxylation does exist, the number of resorbed and released H_2O molecules should increase with T_{max} because the greater temperature and degree of dehydroxylation, the greater the number of undersaturated residual oxygen atoms formed and the greater the number of H_2O molecules that would be required for rehydroxylation (see below). In contrast, the same number of H_2O molecules is released under the medium-temperature treatment independent of T_{max}.

The other characteristic feature of dehydration is that it is time dependent. A decrease of the heating rate to 2ºC/min increases only slightly the number of dehydrated and resorbed H_2O molecules (Figure 6c,d). In contrast, when, during the cooling stage, illite-1*M* was maintained at 300ºC and 250ºC for 1 h at each of these temperatures, weight loss and weight gain increased to 0.35−0.37% (Figure 6c,d). The experimental XRD pattern simulation (Figure 2) and the structural formulae (Table 2) allow the calculation of the amount of H_2O occupying K-free sites in illite interlayers.

According to Środoń *et al*. (1992), the amount of K in illite is under-represented when calculated from chemical analyses. The rationale is that illite has 3D structural disorder and may contain expandable interlayers. Therefore, substitution of Al for Si in the tetrahedral sites adjacent to these interlayers is less than in the tetrahedral sites adjacent to illite interlayers. Środoń *et al*. (1992) showed that for illites and I-S from bentonites, the amount of K in the illite interlayers is constant and equal to 0.89 atoms per $O_{10}(OH)_2$ independent of expandability of I-S.

Let us consider as an example illite-1*M* and $2M_2$ samples. According to diffraction simulation, 90% illite layers are interstratified with 10% smectite layers and $\bar{N}$ and 23, respectively. The mean number of layers in illite fundamental particles ($\bar{n}$) consisting of K-bearing, non-expandable interlayers and providing 3D diffraction effects is related to $\bar{N}$, which is responsible for basal reflection formation and expandability, W_{exp}, by the equation (Drits *et al.*, 1997):

$$\bar{n} = \frac{\bar{N}}{\left(\bar{N}-1\right)\cdot W_{exp}+1}$$

and is equal to 6.78 and 7.19 for illite-1*M* and $2M_2$ samples. The number of K cations in the illite interlayers, C_K, of the illite samples can be calculated using the equation:

$$(\bar{n} - 1)C_K = 0.74\bar{n}$$

where 0.74 is the number of interlayer K cations per $O_{10}(OH)_2$ according to the structural formulae (Table 2). Thus, C_K is equal to 0.87 and 0.86 atoms of K per $O_{10}(OH)_2$. These values are close to 0.89 atoms of K predicted by Środoń *et al*. (1992). Therefore, the number of H_2O molecules in K-free interlayer sites is equal to 0.13 and 0.14 per $O_{10}(OH)_2$ for illite-1*M* and $2M_2$ samples, respectively. These values correspond to 0.58% and 0.63% of the illite-1*M* and $2M_2$ sample weights, respectively, and as such they are still significantly greater than those values (0.35−0.37%) determined for illite-1*M* when cooling was delayed. In contrast, Slonimskaya *et al*. (1978) determined weight loss relating to dehydration of 0.5−0.6%; these values are close to the calculated ones. Because both studies used the same illite samples, we believe that all K-free interlayer sites are occupied by H_2O. It is emphasized that Slonimskaya *et al*. (1978) did not observe weight loss at 300ºC in a true muscovite sample having a K content of close to 1.0 atom per structural unit.

The source of discrepancies can be related to different heating-cooling procedures used in the studies. Slonimskaya *et al*. (1978) measured a weight loss relating to dehydration by maintaining the sample at 300ºC until a constant weight was achieved. In our experiment, a rapid and continuous increase in temperature delayed hydration to 340−360ºC. Similarly, if the heating time at 280−320ºC is prolonged, then all the interlayer H_2O will be liberated. In contrast, if cooling rapidly, as in the current experiments, only some of the interlayer sites available can resorb H_2O molecules.

We have a different interpretation of the hydration mechanism. With experiments achieving a constant weight, Slonimskaya *et al*. (1978) suggested that during each heating stage, H_2O molecules formed during partial dehydroxylation and these molecules are trapped in the illite interlayer cavities and do not leave the structure. However, for long-duration experiments, two successive reactions occur: OH groups form H_2O molecules owing to partial dehydroxylation, which are removed from the structure, but then some H_2O molecules are resorbed in the interlayer.

We do not know what forces compel neutral H_2O molecules to be resorbed into the illite interlayer. However, this hydration reaction is a fact determined experimentally.

There are several possibilities for the source of resorbed H_2O molecules. The H_2O molecules may be mixed with the He carrier gas and the H_2O can enter the furnace from vapor in the room air. A portion of the molecules may be from the dehydroxylation and dehydration reactions.

Dehydroxylation-rehydroxylation reactions in leucophyllite

Several distinct features in the thermal behavior of leucophyllite differ from those of illite. In contrast to illite, the number of H_2O molecules resorbed during cooling and released during heating permanently

increases with cycle number (Figure 7). Second, the number of H_2O molecules resorbed (0.19−0.31%) is significantly greater than that released during heating except for the last two cycles where the values almost coincide. This difference is especially high for the first seven cycles within the interval 360−460ºC where weight loss varies from 0.07 to 0.19% (Figure 7). In the illite-1*M* and $2M_2$ samples, weight loss and increase in this temperature interval are equal and are small (0.06−0.09%, Figure 6c,d). Third, the temperature values of the medium-temperature peaks in leucophyllite (450−460ºC) are significantly greater than those in illite (340−360ºC). Finally, leucophyllite and illite differ in that the temperatures at which the maximum rate of weight increase occurs also differ (~400ºC and 300ºC, respectively).

These observations indicate that the heating-cooling procedure is accompanied by partial rehydroxylation of leucophyllite during each cooling stage. Some of the resorbed H_2O molecules are trapped in the leucophyllite interlayer whereas the majority migrate from the interlayer into the octahedral sheet of the 2:1 layer and reform as OH groups. This model accounts for the observed increase in weight loss and weight gain with cycle number. The greater the temperature and degree of dehydroxylation, the greater the number of H_2O molecules required for rehydroxylation. On the other hand, the observed difference between weight loss and weight gain (Figure 7) originate because heating temperatures were not sufficiently high to provide dehydroxylation of all the newly formed OH groups. Nevertheless, the bond strengths of these newly formed OH groups with the nearest octahedral cations and oxygen atoms of the 2:1 layers are weaker than the bond strengths of the other OH groups which survived the preceding thermal treatments. Therefore the origin of the peaks near 450−460ºC in the mass 18 spectrum is probably related to dehydroxylation of the newly rehydroxylated OH groups. Their dehydroxylation occurs during the last several cycles when both the number of these OH groups and the thermal energy are sufficiently high for this reaction to proceed.

This model is consistent with the results of Heller *et al*. (1962) who showed that partial rehydroxylation occurs easily in montmorillonite where there is low substitution of tetrahedral Al for Si similar to leucophyllite.

Thermal behavior and crystal chemistry

To understand the ability of leucophyllite to rehydroxylate, and in contrast, the lack of this phenomenon in illite, we consider the crystal chemistry of leucophyllite and illite in the natural and dehydroxylated states.

Dehydroxylation of leucophyllite involves only OH loss without accompanying octahedral cation migration, because the $c\cos\beta/a$ values (Muller *et al*., 2000a, 2000b; Tsipursky *et al*., 1985) determined for leucophyllite and its dehydroxylate have almost the same values (0.363*a*). In *trans*-vacant (*tv*) structures, the former octahedral sheet contains five-fold coordinated Al,Mg cations instead of Al,Mg in octahedral coordination (Udagawa *et al*., 1974; Guggenheim *et al*., 1987). The decrease in the cation coordination number results from the reaction between the two adjacent OH groups according to $2(OH) \rightarrow H_2O\uparrow + O_r$. The H_2O molecule migrates out of the structure and the residual oxygen O_r, moves to the same *Z* coordinate position as that of the five-fold coordinated cations. The O_r is located midway between the two closest Al,Mg cations making five-fold coordination.

Pauling's electrostatic principle may be used to estimate the relative stability of *tv* dehydroxylates, following the procedures used by Guggenheim *et al*. (1987). Pauling's principle states that the sum of the bond strengths received by the anion from the nearest coordinating cations should be equal to the valence of this anion. The bond strength is defined as the cation charge divided by the cation coordination number and is expressed in valence units (v.u.). According to the structural formulae, the leucophyllite layer charge is located in the octahedral sheet from the substitution of Mg for Al. Besson and Drits (1997) showed that the octahedral sheet of the same leucophyllite sample in this study contains numerous local structural arrangements in which two adjacent OH groups are bonded with one Al and one Mg, or with two Mg cations. In dehydroxylated 2:1 layers these Al-OH-Mg and Mg-OH-Mg arrangements are reacted to Al-O_r-Mg and Mg-O_r-Mg. Because of the low valence of Mg and the pentagonal coordination of Al and Mg, the residual oxygen atoms should be strongly under-saturated with respect to positive charge. In particular, O_r atoms should receive only 0.8 v.u. or 1 v.u. when they are bonded with two Mg cations or with one Al and one Mg cations, respectively. In addition, five-fold coordination is not suitable for Mg. Thus, after each heating stage, partial dehydroxylation creates local structural sites that destabilize the leucophyllite structure. To provide at least a partial stabilization of the layers, resorbed H_2O molecules migrate first into the interlayer ditrigonal cavities and then to the residual oxygen atoms to form OH groups according to $H_2O + O_r \rightarrow 2(OH)$ during the subsequent cooling stage. The number of under-saturated residual oxygen atoms increase with cycle numbers and therefore the number of resorbed H_2O molecules also increase and are reacted to new-formed OH groups.

It is clear that leucophyllite is more stable than its partial dehydroxylate products and therefore high temperature is required to activate the reaction. Thus, one expects that the rehydroxylation process of the leucophyllite partial dehydroxylate would occur because the source of the structural destabilization is located in the octahedral sheet.

In contrast, the source of the net negative layer charge in the illite-1*M* and $2M_2$ samples (Table 2) is

located in the tetrahedral sheets. The octahedral sheets are almost electrostatically neutral because octahedral sites are occupied mostly by Al. In the dehydroxylated structure, the residual oxygen atoms are under-saturated, receiving 1.2 v.u. whereas oxygen atoms common to the Al pentagons and Si tetrahedra are over-saturated by positive charge receiving 2.2 v.u. A sum of bond strengths received by an O atom common for two Al pentagons and one Al tetrahedron is equal to its valence. In order to compensate the unsatisfied charges of the O_r and O in the dehydroxylate illite structure, the Al cation forms a stronger bond (moves close) to the O_r and weaker bonds (moves away) to the O atoms with summations of 2.2 v.u. (Guggenheim, 1990). Thus, in a partially dehydroxylated illite, a level of undersaturation of residual oxygen atoms and other oxygens coordinating Al cations is significantly lower in comparison with that of the partially dehydroxylated leucophyllite.

In contrast to leucophyllite, the basal oxygen atoms of illite are undersaturated by positive charge owing to Al-for-Si substitution. In addition, in a partially dehydroxylated illite a decrease of bonds between Al cations and the oxygen atoms with a summation of 2.2 v.u. should increase bond strengths between these oxygen atoms and Si, and decrease bond strengths between the Si atoms and the basal oxygens within Si tetrahedra. Resorbed H_2O molecules located in K-free sites in the illite interlayer may create hydrogen bonds with the nearest basal oxygen atoms to promote their local charge compensation. To confirm location of H_2O molecules in the illite interlayers, application of spectroscopic techniques to illite samples subjected to heating-cooling cycles is required.

Problems with interpretation of the low-temperature peak origin

For all samples, low-temperature resorption of H_2O molecules during each cooling stage occurs within close temperature intervals at 80 and 35ºC for illite and between 100 and 35ºC for leucophyllite (Table 4). Similarly, during each heating stage, weight loss starts at 35ºC and quickly reaches a maximum rate. This rate then decreases and is complete at 180–230ºC (Table 3). Therefore, temperatures at which resorption of H_2O molecules starts are significantly lower than those at which dehydration is complete. Probably, resorbed H_2O molecules reconstruct their initial local environments and their removal from the structure requires greater thermal energy than that consumed for resorption of H_2O molecules. For these reasons the weight loss for each sample is independent of cycle number and is reproducible (Figure 6a,b). However, the number of H_2O molecules lost and resorbed during heating-cooling cycles differs for different samples. The illite-1*M* and $2M_2$ show low (0.07–0.08%) weight losses, whereas for leucophyllite-1*M,* low-temperature weight loss is ~2–3 times greater (0.25–0.30%). This difference is not related to H_2O released from smectite interlayers because all the samples have a similar number of expandable interlayers, but different low-temperature weight losses. The H_2O molecules released during the low-temperature heating are probably bound to outer surfaces of mineral particles and any smectite interlayers present.

The actual location and structure of surface centers binding H_2O is not known and we may only assume that these centers are somehow related to specific crystal chemical features of the sample. Additional investigation is needed to understand the nature of the structural centers of bonded H_2O molecules released and resorbed at the low-temperature treatments.

ACKNOWLEDGMENTS

The authors extend special thanks to Dr Steve Guggenheim for valuable comments and suggestions to improve the paper. We also thank the editorial staff and an anonymous referee for their suggestions. Financial support was provided by Chevron and we are grateful to Russell Anderson and Kym Correll for sample preparation. VAD thanks the Russian Foundation of Fundamental Research. We are also grateful to N. Güven and L. Heller-Kallai for useful suggestions.

REFERENCES

Bailey, S.W. (1984) Crystal chemistry of the true micas. Pp. 13–60 in: *Micas* (S.W. Bailey, editor). Reviews in Mineralogy, **13**. Mineralogical Society of America, Washington, D.C.

Besson, G. and Drits, V.A. (1997) Refined relationships between chemical composition of dioctahedral fine-grained mica minerals and their infrared spectra within the OH stretching region. Part I: Identification of the OH stretching bands. *Clays and Clay Minerals*, **45**, 158–169.

Bish, D.L. and Duffy, C.J. (1990) Thermogravimetric analysis of minerals. Pp. 95–157 in *Thermal Analysis in Clay Science* (J.W. Stucki and D.L. Bish, Technical Editors, F.A. Mumpton, Managing Editor). CMS Workshop Lectures, Vol. **3**, The Clay Minerals Society, Bloomington, Indiana.

Drits, V.A. (2003) Structural and chemical heterogeneity of layer silicates and clay minerals. *Clay Minerals*, **38**, 403–432.

Drits, V.A., Besson, G. and Muller, F. (1995) Structural mechanism of dehydroxylation of cis-vacant 2:1 layer silicates. *Clays and Clay Minerals*, **43**, 718–731.

Drits, V.A., Środoń, J. and Eberl, D.D. (1997) XRD measurement of mean crystallite thickness of illite and illite/smectite: Reappraisal of the Kübler index and the Scherrer equation. *Clays and Clay Minerals*, **45**, 461–475.

Emmerich, K., Madsen, F.T. and Kahr, G. (1999) Dehydroxylation behavior of heat-treated and steam-treated homoionic *cis*-vacant montmorillonites. *Clays and Clay Minerals*, **47**, 591–604.

Ferrage, E., Lanson, B., Malikova, N., Plançon, A., Sakharov, B.A. and Drits, V.A. (2005) News insights in the distribution of interlayer H_2O molecules in bi-hydrated smectite from X-ray diffraction profile modeling of *00l* reflections. *Chemistry of Materials*, **17**, 3499–3512.

Grim, R.E. (1968) *Clay Mineralogy: International Series in the Earth and Planetary Sciences* (F. Press, editor). McGraw-Hill Book Company, New York, 596 pp.

Guggenheim, S. (1990) The dynamics of thermal decomposi-

tion in aluminous dioctahedral 2:1 layer silicates: A crystal chemical model. *Proceedings of the 9th International Clay Conference, Vol. 2: Surface chemistry, structure and mixed layering of clays* (V.C. Farmer and Y. Tardy, editors). Strasbourg, France, pp. 99–107.

Guggenheim, S., Chang, H.Y. and Koster van Groos, A.F. (1987) Muscovite dehydroxylation: High-temperature studies. *American Mineralogist*, **72**, 537–550.

Güven, N. (2001) Mica structure and fibrous growth of illite. *Clays and Clay Minerals*, **49**, 189–196.

Heller, L., Farmer, V.C., Mackenzie, R.C., Mitchell, B.D. and Taylor, H.F.W. (1962) The dehydroxylation and rehydroxylation of triphormic dioctahedral clay minerals. *Clay Minerals Bulletin*, **5**, 56–72.

Heller-Kallai, L. and Rozenson, I. (1980) Dehydroxylation of dioctahedral phyllosilicates. *Clays and Clay Minerals*, **28**, 355–368.

Hower, Y. and Mowatt, G.S. (1966) The mineralogy of illites and mixed-layer illite-montmorillonites. *American Mineralogist*, **5**, 825–854.

Jonas, E.C. (1955) *Clays and Clay Minerals* (A. Swineford, editor). National Academy of Sciences – National Resource Council, Washington, publication **395**, p. 66.

Jonas, E.C. and Grim, R.E. (1957) Differential thermal analysis using controlled atmosphere. Pp. 389–403 in: *The Differential Thermal Investigation of Clays* (R.C. MacKenzie, editor). Monograph 2, Mineralogical Society, London.

Koster van Groos, A.F. and Guggenheim, S. (1987) High-pressure differential thermal analysis (HP-DTA) of the dehydroxylation of Na-rich montmorillonite and K-exchanged montmorillonite. *American Mineralogist*, **72**, 1170–1175.

Koster van Groos, A.F. and Guggenheim, S. (1990) Dehydroxylation of Ca- and Mg-exchanged montmorillonite. *American Mineralogist*, **74**, 627–636.

Mackenzie, R.C. (1957) *The Differential Thermal Investigation of Clays.* Monograph **2**, Mineralogical Society, London, 456 pp.

Mackenzie, R.C. (1982) Down-to-earth thermal analysis. Pp. 25–36 in: *Thermal Analysis.* (B. Miller, editor). Wiley Heyden Ltd, Chichester, UK.

Mackenzie, R.C., Walker, G.F. and Hart, R. (1949) Illite from Ballater. *Mineralogical Magazine*, **28**, 704–713.

McCarty, D.K. and Reynolds R.C. (2001) Three-dimensional crystal structures of illite-smectite minerals in Paleozoic K-bentonites from the Appalachian Basin. *Clays and Clay Minerals*, **49**, 24–35.

Muller, F., Drits, V.A., Plançon, A. and Besson, G. (2000a) Dehydroxylation of Fe^{3+}, Mg-rich dioctahedral micas: (I) structural transformation. *Clay Minerals*, **35**, 491–504.

Muller, F., Drits, V.A., Tsipursky, S.I. and Plançon, A. (2000b) Dehydroxylation of Fe^{3+}, Mg-rich dioctahedral micas: (II) cation migration. *Clay Minerals*, **35**, 505–514.

Muller, F., Drits, V.A., Plançon, A. and Robert, J.P. (2000c) Structural transformation of 2:1 dioctahedral layer silicates during dehydroxylation-rehydroxylation reactions. *Clays and Clay Minerals*, **48**, 572–585.

Slonimskaya, M.V., Drits, V.A., Finko, V.I. and Salyn, A.L. (1978) The nature of interlayer water in fine-dispersed muscovites. *Izvestiya Akademii Nauk SSSR, seriya geologicheskaya*, **10**, 95–104 (in Russian).

Sokolova, T.N., Drits, V.A., Sokolova, A.L. and Stepanova, K.A. (1976) Structural and mineralogical characteristics and formation conditions of leucophyllite from salt deposits. *Litologiya I poleznie iscopaemie*, **26**, 80–95 (in Russian).

Środoń, J., Elsass, F., McHardy, W.J. and Morgan, D.J. (1992) Chemistry of illite-smectite inferred from TEM measurements of fundamental particles. *Clay Minerals*, **27**, 137–158.

Tsipursky, S.I., Kameneva, M.Y. and Drits, V.A. (1985) Structural transformation of Fe^{3+}-containing 2:1 dioctahedral phyllosilicates in the course of dehydration. *5thMeeting of the European Clay Groups* (J. Konta, editor) Prague, pp. 569–577.

Udagawa, S., Urabe, K. and Hasu, H. (1974) The crystal structure of muscovite dehydroxylate. *Japanese Association of Mineralogy, Petroleum and Economic Geology*, **69**, 381–389.

Wardle, R. and Brindley, G.W. (1972) The crystal structures of pyrophyllite-1Tc and of its dehydroxylate. *American Mineralogist*, **57**, 732–750.

(*Received 23 March 2006; revised 8 August 2006; Ms. 1156; A.E. Will P. Gates*)